PHYSICAL REVIEW A **79**, 020102(R) (2009)

Numerical studies of Lifshitz interactions between dielectrics

S. Pasquali and A. C. Maggs
Laboratoire de Physico-Chime Théorique, Gulliver, CNRS-ESPCI, 10 rue Vauquelin, 75231 Paris Cedex 05, France
(Received 28 January 2008; published 18 February 2009)

We study numerically the fluctuation-derived interaction between dielectrics in both two and three dimensions. We demonstrate how sparse matrix factorizations enable one to study torsional interactions in three dimensions. In two dimensions we study the full crossover between nonretarded and retarded interactions as a function of separation. We use constrained factorizations in order to measure the interaction of a particle with a rough dielectric surface and compare with a scaling argument.

DOI: 10.1103/PhysRevA.79.020102 PACS number(s): 12.20.Ds, 42.50.Wk, 02.70.−c, 42.50.Ct

Dispersion forces have as their origin the fluctuations of polarization in materials coupled to the long-range electrodynamic interaction described by Maxwell's equations. They were first treated in a study of the interaction between fluctuating classical dipoles [1]. The introduction of quantum fluctuations [2] accounted for the long-range, $1/r^6$, part of the interaction in most materials. Later it was demonstrated [3] that retardation modifies the interactions in an important manner, leading to a decay in the interaction which is asymptotically $1/r^7$ at zero temperature. Further advances [4] showed how to formulate the interactions in terms of the dielectric response of materials. Overviews with many references to theoretical and experimental developments are to be found in [5–7]. Dispersion interactions are the dominant long-range interaction between neutral surfaces.

While the analytic basis of the theory is largely established, its application is difficult in many interesting geometries. One is constrained to work with perturbative expansion about exactly solvable geometries [8] or use *ad hoc* schemes such as the proximity force approximation. Only a few geometries have been attacked with exact analytic techniques [9]. Recently several attempts have been made to study numerically the interactions by using methods from modern computational science, including fast multigrid lattice solvers [10], in order to calculate Green functions and forces, or the use of discretized determinants to determine free energies [11,12].

In this article we will present a series of techniques which enable one to evaluate the interaction between dielectric bodies in propagating, vectorial electrodynamics; our previous work only considered cases which could be mapped onto a static, scalar potential [11,12]. First, we calculate the torsional potential between two three-dimensional bodies in the retarded regime, using discretized Maxwell's equations. The torque has recently received the attention of experimentalists [13,14]; we refer the reader to their papers for detailed estimates of physical parameters.

A important point that we wished to examine with our study of torques is the numerical stability of results in the face of interpolations which vary due to incommensurate motion of a body with respect to an underlying lattice. Previous lattice studies have only considered parallel translation of bodies, which hides many of the difficulties due to the variation of the self-energy of bodies which have been discretized to a lattice.

For more detailed studies we present results for two-dimensional systems. This allows us to study the crossover between the near- and far-field regimes and also to measure the interaction between a particle and a rough surface. With these two-dimensional systems we implement strategies which increase the efficiency of simulations, at the same time decreasing the sensitivity of the results to numerical round-off errors.

In three dimensions we discretize Maxwell's equations to a cubic Yee lattice [15], lattice constant $a=1$, associating the electric degrees of freedom with the links; magnetic degrees of freedom are localized on the faces of the lattice. We remind the reader that the finite-difference approximation to the $\boldsymbol{\nabla}\times$(operator), here designated Curl, maps the electric field on four links surrounding the face of the cube to the magnetic field. The adjoint operator Curl* maps fields from faces to links. We find

$$\frac{\partial \mathbf{H}}{\partial t} = -c\ \mathrm{Curl}\ \mathbf{E}, \quad \frac{\partial \mathbf{D}}{\partial t} = c\ \mathrm{Curl}^*\ \mathbf{H}.$$

The importance of clearly distinguishing the two operators will become apparent when we discuss the two-dimensional case below. We use Heaviside-Lorentz units in which Maxwell's equations are directly parametrized by the speed of light in vacuum, c.

From these two equations Lifshitz theory [4] shows that the free energy of interaction between dielectric bodies is found from the imaginary-time wave equation for the vector potential in the temporal gauge where $\mathbf{E}=-\dot{\mathbf{A}}/c$ and $\phi=0$:

$$\left\{\frac{\epsilon(\mathbf{r},i\omega)\omega^2}{\hbar^2c^2} + \mathrm{Curl}^*\ \mathrm{Curl}\right\}\mathbf{A} = \mathcal{D}_A\mathbf{A} = 0.$$

Alternatively one introduces a magnetic formulation and works with a potential such that $\mathbf{H}=\dot{\mathbf{G}}/c$ and considers the wave equation

$$\left\{\frac{\omega^2}{\hbar^2c^2} + \mathrm{Curl}\ \frac{1}{\epsilon(\mathbf{r},i\omega)}\ \mathrm{Curl}^*\right\}\mathbf{G} = \mathcal{D}_G\mathbf{G} = 0.$$

In our work we always consider the differences in free energy between pairs of configurations; we thus avoid a full account of the self-energy variations of dielectric media [11]. The free-energy difference between two configurations 1 and 2 is found from

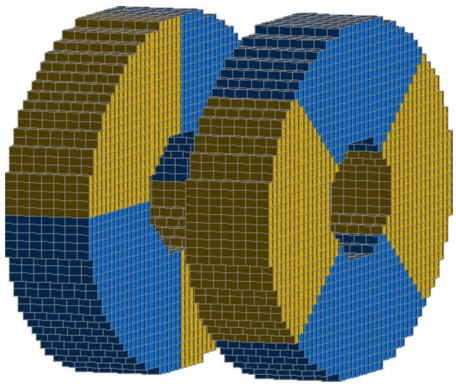

FIG. 1. (Color online) A pair of structured dielectric rings. Each quadrant has different dielectric properties.

$$U^{1,2} = \int_0^\infty \frac{d\omega}{2\pi} \{\ln \det \mathcal{D}^1(\omega) - \ln \det \mathcal{D}^2(\omega)\} \qquad (1)$$

for either choice of wave operator, $\mathcal{D}_A$ or $\mathcal{D}_G$; while self-energy contributions are different in the two formulations, we have verified with our codes that both give the same result for the interactions between bodies.

We perform the frequency integration in Eq. (1) by changing the integration variables to z, where $\omega = \alpha z/(1-z)$, with $0 < z < 1$. The parameter α is chosen so that the major features in the integrand occur for values of z near $1/2$. We then use N_g-point Legendre-Gauss quadrature to replace the integral by a weighted sum over discrete frequencies. We evaluate determinants by finding the Cholesky factorization L_D of $\mathcal{D}(\omega)$ such that L_D is lower triangular [16] and $L_D L_D^T = \mathcal{D}(\omega)$. Then $\ln \det \mathcal{D}(\omega) = 2\Sigma_i \ln(L_{D,i,i})$.

When we examine the detailed structure of Maxwell's equations discretized to $V = L^3$ sites in three dimensions, we discover that the Curl operator is a matrix of dimension $3V \times 3V$. The major technical difficulty comes from the fact that the matrices we work with have dimensions which are very large, $\sim 10^6 \times 10^6$. Standard dense matrix methods lead to enormous storage requirements. We thus worked exclusively with sparse matrix factorizations.

We now calculate the torque between two parallel rings centered on a common axis, Fig. 1. Each ring is divided into quadrants with alternating dielectric properties. We take permittivities which are independent of frequency, corresponding to the full retarded regime [4] with $\epsilon_1(\omega) = 5$ and $\epsilon_2(\omega) = 10$; the space around the rings is a vacuum with $\epsilon_r = 1$. As the rings are rotated, the interface between the dielectric materials, as interpolated to the lattice, undergoes some rearrangement changing the self-energy of the rings. We thus perform two runs. The first run of a single rotating ring determines this variation in the self-energy. The second run with both rings allows one to measure the interaction energy by subtraction.

We worked with two systems of dimensions $V = 45^3$ and $V = 63^3$, Fig. 2. The graph of the interaction energy as a function of angle is somewhat triangular in shape between $\pi/8$ and $3\pi/8$, an effect which is strengthened when the gap is reduced. The fluctuations in the curve about the expected

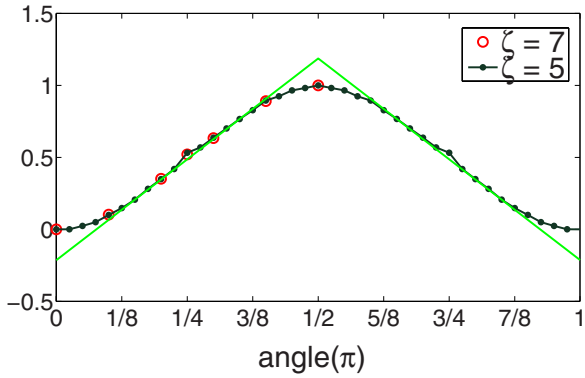

FIG. 2. (Color online) Interaction energy as a function of angle as a ring of Fig. 1 rotates. In the central parts of the curve, the torque is almost independent of the angle. Two systems, box size $L = 9\zeta$, inner radius ζ, outer radius 3ζ, and separation ζ for $\zeta = 5$ and $\zeta = 7$. All numerical work performed with a Xeon-5140 workstation. If we scale our results so that the separation between the rings is 0.5 μm, then we find that the amplitude of the interaction is equal to 8.6×10^{-3} eV. The energy for other systems sizes is found by noting that for constant aspect ratios of the bodies it scales inversely with the separation.

linear behavior give an idea of the errors coming from irregularities of the interpolation of the disks to the lattice. This irregularity is particularly clear for the points at $\pi/4$ and $3\pi/4$. From our previous experience of errors in discretizing thermal interactions [11], we expect that systematic errors coming from the lattice should be smaller than 4% for this separation between the bodies. Comparison between the two systems presented here confirms this point.

We now turn to two-dimensional electrodynamics where we study larger system sizes in order to follow the crossovers between qualitatively different regimes. In three dimensions the two formulations in terms of $\mathcal{D}_A$ and $\mathcal{D}_G$ are largely equivalent. In two-dimensional electrodynamics this is no longer the case. Consider an electrodynamic system in which there are two components of the electric field in the x-y plane; the magnetic field then has just a single component in the z direction. The Curl operator becomes a *rectangular matrix* of dimensions $V \times 2V$ where now $V = L^2$. The standard formulation in terms of the vector potential gives rise to an operator $\mathcal{D}_A$ of dimensions $2V \times 2V$; the alternative formulation in terms of $\mathcal{D}_G$ leads to determinants of dimensions $V \times V$; the size of the matrix that we must work with is smaller in the $\mathcal{D}_G$ formulation. We used D_G in the following numerical work, having checked that we obtain equivalent results.

We started by measuring the crossover between the short-range nonretarded interaction to the long-range retarded force. We studied a pair of dielectric particles described by the single-pole approximation to the dielectric constant:

$$\epsilon(\omega) = 1 + \frac{\chi}{1 - \omega^2/\omega_0^2},$$

where χ is the zero-frequency electric susceptibility. The interaction is retarded for separations $D \gg c/\omega_0$, nonretarded for $D \ll c/\omega_0$. We note that the analytic form of the dielectric

response corresponds to an optical dispersion with an absorbing spectral line at ω_0. More general dielectric functions are treated as easily as this particular case. Birefringence is introduced by use of a tensor variable $\epsilon_{i,j}(\omega)$.

We measured the interaction between two dielectric particles in a square, periodic cell of dimensions $L\times L$ using SuiteSparse [17] to perform both the ordering and the factorization of the matrices. The particles are implemented by modifying the dielectric response on the four links incident on a site of the network defining the center of the particle. We placed a first particle at the origin and considered two possible positions of a second particle to calculate a free-energy difference using Eq. (1). The first results were disappointing—rather small systems ($L=50$) were sensitive to numerical round-off errors. In a large system there is an extensive self-energy $\sim L^2$. Pair interactions calculated as the difference between two large numbers are unreliable. This large self-energy is an echo of the true ultraviolet divergences that occur in the continuum theory.

We avoided this problem by separating the free-energy contributions from the neighborhood of the three interesting sites and the rest of the system. We did this by introducing a blockwise factorization of $\mathcal{D}$ that enabled us to both solve the round-off problem while reusing much of the numerical effort need to generate the Cholesky factors, thus improving the efficiency of the code. We now write the symmetric matrix from the wave equation in block form

$$\mathcal{D}=\begin{pmatrix} X & Y \\ Y^T & Z \end{pmatrix}.$$

Its determinant is $\det(\mathcal{D})=\det(X)\det(S)$, where the Schur complement $S=Z-Y^TX^{-1}Y$ [18]. We group sites so that the great majority is within block X and sites that we are interested in are in block Z. It is the term in $\det(X)$ that the gives the large extensive free energy which caused our numerical problems. It is independent of the properties of our test particles. All the interesting information on energy differences is in the Schur complement S.

We start by finding the Cholesky factorization of X, L_x. The Schur complement is calculated by solving the triangular equations $L_xU=Y$ by forward substitution, then calculating $S=Z-U^TU$. Our separation of energies into an extensive constant and a small set of interacting sites allows us to study the interaction of systems of sizes up to $L=2000$ before round-off becomes a problem.

In order to generate data we generalized the method to a three level scheme: first, collect the set of sites (here ~ 100) of all the separations required to generate a curve into block Z and form the Schur complement, forming a small effective theory for all these remaining sites. Within the smaller matrix that has been generated, we again reorder to successively put each interesting set of variables in the bottom-right corner of the effective theory and find the Schur complement of these remaining variables. We can then calculate interactions between the particles while minimizing round-off errors.

We remind the reader that in two dimensions the electrostatic potential is logarithmic between two charges and that dipole-dipole fluctuations lead to van der Waals interactions

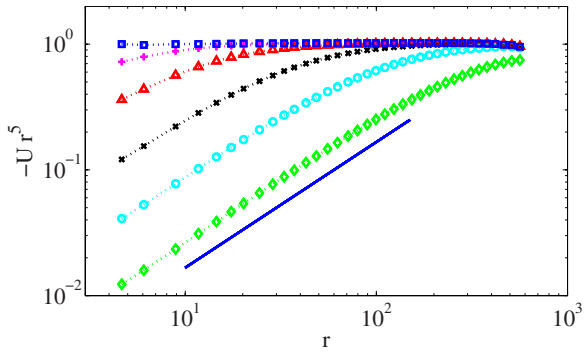

FIG. 3. (Color online) Scaled interaction free energy $-Ur^5$ for a pair of dielectric particles [$\epsilon(0)=8$] in a box of dimensions 2000×2000 as a function of separation. Curves from top to bottom correspond to $\omega_0/c=10,0.3,0.1,0.03,0.01$ 0.003. For large ω_0/c, Ur^5 is constant, □. For smaller ω_0/c we see both retarded and nonretarded interactions. Solid line corresponds to $U_{vdw}\sim 1/r^4$. 10 GB for the Cholesky factor. Six hours of calculation. $N_g=25$.

decaying as $U_{vdw}=1/r^4$. As in three dimensions, retardation leads to an accelerated decay so that the retarded interaction varies as $U_c\sim 1/r^5$. In our simulations we used values of ω_0/c varying from 0.003 to 10, Fig. 3. We determined the energy of interaction of particles, U, as a function of separation r while moving the second particle in the simulation cell out to $(L/5,L/5)$; the zero of energy is calculated for two particles separated by $(L/2,L/2)$. We scale out the retarded behavior, plotting $-U(r)r^5$. We see that for the largest ω_0/c the interactions are retarded for all separations, □. For the smaller values of ω_0/c the interaction varies as $1/r^4$. In the scaled curve this gives the linear rise clearly visible in the figure, ◇. For $0.01<\omega_0/c<0.1$ both the near- and far-field behaviors are clearly displayed within a single sample, permitting the detailed study of crossover phenomena with frequency-dependent dielectric behavior. No assumptions of symmetry are made in the calculation; the method can be used with bodies of arbitrary geometry. For even the smallest separation of (1,1), the data for the interaction energy fall on the scaled curve, showing that the discretization to a lattice gives good accuracy at even the smallest separations. We did not measure the interaction for a separation of (1,0), which leads to overlaping particles.

We now turn to the interaction of a dielectric particle with a rough surface, Fig. 4. We generated surfaces as realizations of solid-on-solid random walks on a lattice. Approximately half of the simulation box contains dielectric material with $\epsilon=8$ and $\omega_0=\infty$; the rest of the box has $\epsilon=1$. We measure the interaction with a test particle using the Schur complements to perform a single large factorization per frequency for each sample. We generated 1000 rough surfaces and measured both $\langle U\rangle$ and the variance as a function of separation.

We understand the results, Fig. 5, with a scaling argument. When the particle is a distance r from the surface, the interaction is dominated by a front of length r along the surface. Since the surface is a random walk, its average position is displaced by $\delta r\sim\pm r^{1/2}$ compared to the flat surface. The interaction between a smooth surface and a particle varies as $U_s\sim 1/r^3$ in the retarded regime. The interaction of the particle should thus be $U\sim 1/(r+\delta r)^3$. If we expand to

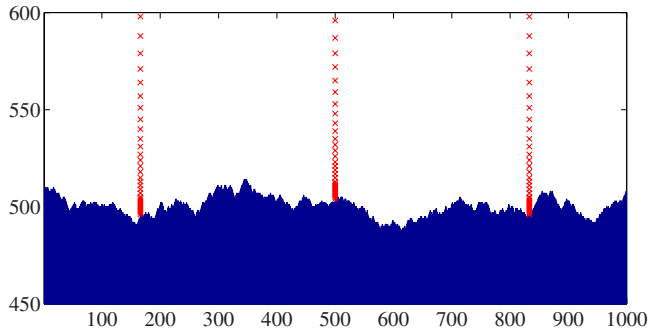

FIG. 4. (Color online) Realization of rough interface and set of measurement positions, ×, for the interaction energy which will be separated into block Z. Anisotropic horizontal and vertical scales.

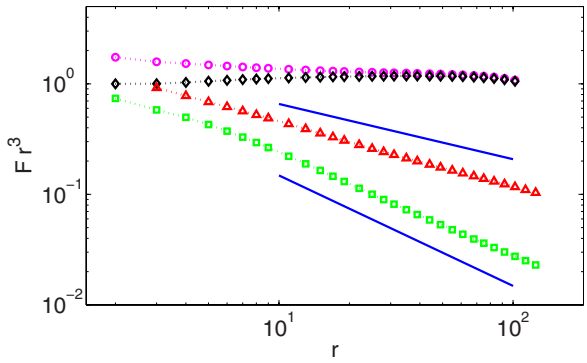

FIG. 5. (Color online) (1) ○, $-\langle U\rangle r^3$, averaged interaction between dielectric particle and rough dielectric surface. (2) ◇, $-U_s r^3$, interaction between particle and flat surface. (3) △, $\sigma_u r^3$, variance of interaction for rough surfaces. (4) □, $\delta U r^3$, difference in mean interaction energy between a flat and a rough surface. Solid lines: $r^{-3.5}$ and r^{-4}. $L=1000$. Two weeks of simulation time. Cholesky factor 2.5 GB. $N_g=20$.

first order, we find that the variance of the interaction should scale as (△) $\sigma_u \sim r^{-3.5}$, while the second-order expansion gives a shift in the mean potential, $\langle U\rangle$, which varies as (□) $\delta U \sim 1/r^4$. The numerical data are compatible with this scaling [19].

We have demonstrated the power of direct methods from linear algebra when applied to the study of dispersion forces. In three dimensions we have measured interactions in experimentally realizable geometries, though system sizes are still too small to accurately measure crossovers between different scaling regimes. Improvements in lattice artifacts can also be expected if one adapts smoothing algorithms for electrostatics that are widely used in atomistic simulations of charged systems [20]. In two dimensions quite detailed measurements are possible; we believe that this will lead to fruitful interactions with analytic calculations. We note that Cholesky factorizations are standard components in many engineering and hydrodynamic codes. On large parallel computers efficient, implementations are available, allowing one to scale the present methods to much larger systems.

This work was financed in part by Volkswagenstiftung.

[1] W. H. Keesom, Phys. Z. **22**, 129 (1921).
[2] F. London, Trans. Faraday Soc. **33**, 8 (1937).
[3] H. B. G. Casimir and D. Polder, Phys. Rev. **73**, 360 (1948).
[4] I. D. Dzyaloshinskii, E. M. Lifshitz, and L. P. Pitaevskii, Sov. Phys. Usp. **4**, 153 (1961).
[5] J. Mahanty and B. Ninham, *Dispersion Forces* (Academic Press, New York, 1976).
[6] M. Bordag, U. Mohideen, and V. M. Mostepanenko, Phys. Rep. **353**, 1 (2001).
[7] K. A. Milton, J. Phys. A **37**, R209 (2004).
[8] T. Emig, A. Hanke, R. Golestanian, and M. Kardar, Phys. Rev. A **67**, 022114 (2003).
[9] T. Emig, A. Hanke, R. Golestanian, and M. Kardar, Phys. Rev. Lett. **87**, 260402 (2001).
[10] A. Rodriguez, M. Ibanescu, D. Iannuzzi, J. D. Joannopoulos, and S. G. Johnson, Phys. Rev. A **76**, 032106 (2007).
[11] S. Pasquali, F. Nitti, and A. C. Maggs, Phys. Rev. E **77**, 016705 (2008).
[12] S. Pasquali and A. C. Maggs, J. Chem. Phys. **129**, 014703 (2008).
[13] F. Capasso, J. N. Munday, D. Iannuzzi, and H. B. Chan, IEEE J. Sel. Top. Quantum Electron. **13**, 400 (2007).
[14] C.-G. Shao, A.-H. Tong, and J. Luo, Phys. Rev. A **72**, 022102 (2005).
[15] K. S. Yee, IEEE Trans. Antennas Propag. **14**, 302 (1966).
[16] D. Irony, G. Shklarski, and S. Toledo, FGCS, Future Gener. Comput. Syst. **20**, 425 (2004).
[17] T. A. Davis, *Direct Methods for Sparse Linear Systems* (SIAM, Philadelphia, 2006).
[18] G. H. Golub and C. F. V. Loan, *Matrix Computations* (Johns Hopkins University Press, Baltimore, 1983).
[19] H. Li and M. Kardar, Phys. Rev. Lett. **67**, 3275 (1991).
[20] A. C. Maggs, Phys. Rev. E **72**, 040201 (2005).